PHYSICAL REVIEW B VOLUME 23, NUMBER 9 1 MAY 1981

Mössbauer absorption and emission study of dilute Fe^{2+} impurities in cubic ZnS. Observation of metastable electronic levels.

II. Dynamical Jahn-Teller effect study

P. Bonville, C. Garcin, A. Gérard,* P. Imbert, and G. Jéhanno
Service de Physique du Solide et de Résonance Magnétique, Centre d'Etudes Nucléaires de Saclay, 91191 Gif-sur-Yvette Cedex, France

(Received 28 May 1980)

In the Mössbauer source ZnS:^{57}Co the two excited spin-orbit triplets Γ_4 and Γ_5 of Fe^{2+} behave as metastable levels after being populated by the preceding nuclear decay. They contribute two slow relaxation quadrupole doublets to the emission spectra near zero kelvin. Both quadrupole splittings are reduced by the dynamical Jahn-Teller effect, but in very different ways: the reduction factors are, respectively, $q(\Gamma_4) \simeq 0.92$ and $q(\Gamma_5) \simeq 0.40$. These factors are interpreted by means of a coherent vibronic model where the low-energy TA(L) phonon of ZnS ($\hbar\omega \sim 70$ cm^{-1}), which contributes a Γ_3 vibrational mode, is coupled to the ^5E state of Fe^{2+} with a Jahn-Teller energy $E_{JT} \simeq 14$ cm^{-1}. The covalency reduction of the spin-orbit parameter λ is found to be less important for Fe^{2+} in ZnS ($\lambda = -88.4 \pm 1.6$ cm^{-1}) than for Fe^{2+} in CdTe ($\lambda \simeq -79$ cm^{-1}). The isomer-shift values of the Γ_1, Γ_4, and Γ_5 contributions are not identical because of different second-order Doppler shift values in these vibronic levels.

I. INTRODUCTION

Optical studies[1-3] of Fe^{2+} in the cubic phase of ZnS have shown that there is no important Jahn-Teller coupling in the orbital ground state ^5E and the observed spectra can be accounted for, to a first approximation, using a crystal-field model and spin-orbit coupling.

However, Ham and Slack[3] mentioned that the reduction in the observed spin-orbit splitting relative to the value obtained for the free ion may be due to the combined effects of covalency and a weak Jahn-Teller coupling within the ^5E state. Some evidence in fact indicates that a non-negligible Jahn-Teller effect is likely to exist. The far-infrared absorption study of Vallin, Slack, and Bradley[2] has shown that the spin-orbit levels are not exactly equidistant as predicted by the second-order perturbation treatment of $\lambda\vec{L}\cdot\vec{S}$. Now the exact treatment of $\lambda\vec{L}\cdot\vec{S}$ within the combined ^5E and $^5T_2$ multiplets also cannot account for the fact that the energy difference $E(\Gamma_3) - E(\Gamma_4) = 12.5$ cm^{-1} is smaller than the energy difference $E(\Gamma_4) - E(\Gamma_1) = 15.0$ cm^{-1}, whereas such an effect can result from the Jahn-Teller coupling. Moreover, the electric dipole oscillator strength parameter C_E, as measured from the optical transition $\Gamma_1 \rightarrow \Gamma_5$, can hardly be accounted for without some Jahn-Teller coupling within the ^5E state of Fe^{2+}.[2]

In order to obtain more information concerning this coupling, Ham suggested carrying out a Mössbauer study of the quadrupole interaction in the first excited spin-orbit level Γ_4 of Fe^{2+}, as this interaction should be reduced by a possible dynamical Jahn-Teller effect.[4] While the Mössbauer absorption experiments on the system ZnS:^{57}Fe failed to show any measurable quadrupole interaction because of relaxation averaging, the emission experiments on the source ZnS:^{57}Co gave important and unexpected results (Part I, preceding paper). The two excited spin-orbit triplets Γ_4 and Γ_5 of Fe^{2+}, after being populated by the preceding nuclear decay, contribute two slow-relaxation quadrupole doublets to the emission spectra near zero kelvin. Such an observation appeared to be particularly interesting from the point of view of the Jahn-Teller coupling. First, the hyperfine parameters of the levels Γ_4 and Γ_5 are separately measurable. One of these parameters, the quadrupole splitting, enables the Jahn-Teller reduction factor q to be evaluated for both of the levels. In addition, another parameter, the isomer-shift value, which includes the second-order Doppler shift, gives information about the kinetic energy of the emitting ^{57}Fe nucleus in each vibronic state.

The present paper deals with the interpretation of the ZnS:^{57}Co Mössbauer emission spectra in terms of the dynamical Jahn-Teller coupling. In Sec. II the observed reduction factors $q(\Gamma_4)$ and $q(\Gamma_5)$ are discussed; their interpretation is shown to require a more complex vibronic model than the simplified treatment used by Ham in Ref. 4, where the spin-orbit separation was neglected in comparison with the vibrational energies. In Sec. III the vibronic calculation is developed following the model used by Vallin to interpret the optical data of Fe^{2+} in CdTe.[5] This model is shown to account for the experimental values of $q(\Gamma_4)$ and $q(\Gamma_5)$ as well as for the optically measured energy levels. Extensions of the calculation to the case of strong strains and of applied magnetic fields are given in Sec. IV. The origin of the isomer shift differences between the various Fe^{2+} components in the emission spectra is discussed in Sec. V. The coherence of the interpretation, especially in view of the assignment of the internal quadrupole doublet to the level Γ_5, is examined in the conclusion (Sec. VI), where possible extensions of this work are also discussed.

II. JAHN-TELLER REDUCTION FACTORS—VIBRONIC MODELS

As described in the preceding paper (Part I, Sec. V B) the Mössbauer emission spectrum of the Fe^{2+} ions in ZnS, at 1.3 K, is made up of three parts: one central line due to the ground-state spin-orbit level Γ_1, and two quadrupole doublets, respectively, due to the excited spin-orbit triplets Γ_4 and Γ_5.

Following Ham's predictions,[4] the presence of a weak or moderate dynamical Jahn-Teller effect in the orbital ground state ^5E of Fe^{2+} should lead to a reduction by a common factor q ($\frac{1}{2} < q < 1$) of both the spin-orbit splitting and the quadrupole interaction in the triplet Γ_4 (or in the triplet Γ_5). The value of the quadrupole interaction in both triplets should then be

$$\Delta E_Q = 6q\,|C_E| \text{ with } C_E = \tfrac{1}{7}\langle r^{-3}\rangle e^2Q/[I(2I-1)]$$

(Part I, Sec. III).

However the observed quadrupole splittings are very different for Γ_4 and Γ_5 [$\Delta E_Q(\Gamma_4) = 3.00 \pm 0.03$ mm s^{-1}; $\Delta E_Q(\Gamma_5) = 1.31 \pm 0.04$ mm s^{-1}], which evidences different $q(\Gamma_4)$ and $q(\Gamma_5)$ reduction factors.

In order to deduce these reduction factors from the observed values $\Delta E_Q(\Gamma_4)$ and $\Delta E_Q(\Gamma_5)$, we needed an independent evaluation of the quantity $6|C_E|$ which represents the maximum quadrupole splitting observable in a distorted site in the same matrix. Rather than using a direct calculation of C_E which would require the evaluation of the covalency modified $\langle r^{-3}\rangle$ value, we preferred deriving $6|C_E|$ from the actual quadrupole interactions in distorted sites in ZnS resulting from pair effects ($Fe^{2+}-Fe^{2+}$ or $Fe^{2+}-Cd^{2+}$ pairs[6]), and we adopted the value $6|C_E| = 3.27 \pm 0.03$ mm s^{-1}.[7] Using this value and the measured values of $\Delta E_Q(\Gamma_4)$ and $\Delta E_Q(\Gamma_5)$, we found $q(\Gamma_4) = 0.917 \pm 0.020$ and $q(\Gamma_5) = 0.40 \pm 0.02$.

The large difference between $q(\Gamma_4)$ and $q(\Gamma_5)$ shows that the vibrational energy involved in the Jahn-Teller coupling is not much larger than the spin-orbit separation, which is contrary to the approximation made by Ham in Ref. 4.

In the neighboring system CdTe:Fe^{2+} the characteristics of the far-infrared absorption spectra[8]—and particularly the existence of extra lines not predicted by the crystal-field and spin-orbit theory—led Vallin to propose another model.[5] The particularity of CdTe is that the critical points in the TA phonon branch are so low as to lie among the spin-orbit levels of Fe^{2+}, so that the Jahn-Teller coupling with some of these vibrational modes strongly perturbs the electronic levels and also introduces new optical transitions. In Vallin's calculation the Jahn-Teller interaction is supposed to occur mainly with the TA(L) phonon of the matrix, which contributes a Γ_3 vibrational mode and thus presents the correct symmetry for participating in a coupling with the ^5E state of Fe^{2+}.

Although the TA(L) phonon has a higher energy in ZnS than in CdTe [respectively, $\hbar\omega = 70$ (Ref. 3) and 36 cm^{-1} (Ref. 5)], this energy remains comparable to the overall spin-orbit separation of the ^5E state of Fe^{2+}. Using Vallin's model, we show in the next section that the Jahn-Teller coupling with this mode not only accounts for the very different values of $q(\Gamma_4)$ and $q(\Gamma_5)$ observed, but also accounts for the optically measured energies of the levels Γ_4, Γ_3, and Γ_5.

III. CALCULATION OF THE JAHN-TELLER COUPLING

In order to calculate the effects of the vibronic coupling on the ^5E state of ZnS:Fe^{2+} we follow the main steps of Vallin's calculation for CdTe:Fe^{2+}.[5,9]

A. Spin-orbit levels of ^5E

The spin-orbit Hamiltonian $H_{so} = \lambda\vec{L}\cdot\vec{S}$, to the second order of perturbation theory, gives five equally spaced spin-orbit levels in the ^5E orbital state. The common separation is

$$\delta_{so} = 6(\lambda^2/\Delta + \rho) \tag{1}$$

(see Part I, Sec. III). The spin-orbit wave functions (Table I) span the irreducible representations given by the direct product

$$\Gamma_3 \times (\Gamma_3 + \Gamma_5) = \Gamma_1 + \Gamma_2 + \Gamma_3 + \Gamma_4 + \Gamma_5$$

and they are obtained from the tables of coupling coefficients for the T_d group given by Koster *et al.*[10]

TABLE I. Spin-orbit and vibrational wave functions with corresponding irreducible representations and energies. In the kets such as $|\theta\epsilon\rangle$, the first label denotes the orbital state, the second label the spin state; the correspondence with spherical harmonics is, for E or Γ_3, $|\theta\rangle = Y_2^0$, $|\epsilon\rangle = (1/\sqrt{2})(Y_2^2 + Y_{-2}^{-2})$, and for T_2 or Γ_5, $|\xi\rangle = (i/\sqrt{2})(Y_2^1 + Y_2^{-1})$, $|\eta\rangle = -(1/\sqrt{2})(Y_2^1 - Y_2^{-1})$, and $|\zeta\rangle = (i/\sqrt{2})(Y_2^2 - Y_2^{-2})$. The vibrational wave functions are given for 0, 1, and 2 phonons.

Spin-orbit wave functions	Energy
$(\Gamma_1) = (1/\sqrt{2})(\lvert\theta\theta\rangle + \lvert\epsilon\epsilon\rangle)$	0
$(\Gamma_{4x}) = -(\sqrt{3}/2)\lvert\theta\xi\rangle - (1/2)\lvert\epsilon\xi\rangle$	δ_{so}
$(\Gamma_{4y}) = (\sqrt{3}/2)\lvert\theta\eta\rangle - (1/2)\lvert\epsilon\eta\rangle$	δ_{so}
$(\Gamma_{4z}) = \lvert\epsilon\zeta\rangle$	δ_{so}
$(\Gamma_{3\theta}) = (1/\sqrt{2})(-\lvert\theta\theta\rangle + \lvert\epsilon\epsilon\rangle)$	$2\delta_{\text{so}}$
$(\Gamma_{3\epsilon}) = (1/\sqrt{2})(\lvert\theta\epsilon\rangle + \lvert\epsilon\theta\rangle)$	$2\delta_{\text{so}}$
$(\Gamma_{5\xi}) = -(1/2)\lvert\theta\xi\rangle + (\sqrt{3}/2)\lvert\epsilon\xi\rangle$	$3\delta_{\text{so}}$
$(\Gamma_{5\eta}) = -(1/2)\lvert\theta\eta\rangle - (\sqrt{3}/2)\lvert\epsilon\eta\rangle$	$3\delta_{\text{so}}$
$(\Gamma_{5\zeta}) = \lvert\theta\zeta\rangle$	$3\delta_{\text{so}}$
$(\Gamma_2) = (1/\sqrt{2})(\lvert\theta\epsilon\rangle - \lvert\epsilon\theta\rangle)$	$4\delta_{\text{so}}$

Vibrational wave functions	Energy
$(\Gamma_1)_0 = F_\theta^0 F_\epsilon^0$	0
$(\Gamma_{3\theta})_1 = F_\theta^1 F_\epsilon^0$	$\hbar\omega_e$
$(\Gamma_{3\epsilon})_1 = F_\theta^0 F_\epsilon^1$	$\hbar\omega_e$
$(\Gamma_1)_2 = (1/\sqrt{2})(F_\theta^2 F_\epsilon^0 + F_\theta^0 F_\epsilon^2)$	$2\hbar\omega_e$
$(\Gamma_{3\theta})_2 = (1/\sqrt{2})(-F_\theta^2 F_\epsilon^0 + F_\theta^0 F_\epsilon^2)$	$2\hbar\omega_e$
$(\Gamma_{3\epsilon})_2 = F_\theta^1 F_\epsilon^1$	$2\hbar\epsilon_e$

B. Vibrational wave functions

The vibrational Hamiltonian is that of the two-dimensional harmonic oscillator

$$H_{\text{vib}} = \left(\frac{1}{2\mu}\right)[P_\theta^2 + P_\epsilon^2 + \mu^2\omega_e^2(Q_\theta^2 + Q_\epsilon^2)] \ , \tag{2}$$

where P_θ and P_ϵ are momenta conjugate to the lattice distortion coordinates Q_θ and Q_ϵ which transform as Γ_3 and contribute to the Jahn-Teller coupling with the orbital doublet ^5E. The effective energy $\hbar\omega_e$ of these modes is taken to be 70 cm^{-1}, which is the energy of the mode TA(L) in ZnS.[3]

The vibrational eigenfunctions of Eq. (2) are the products $F_\theta^n F_\epsilon^m$ of the simple-harmonic-oscillator wave functions $F_\theta^n \equiv F^n(Q_\theta)$ and $F_\epsilon^m \equiv F^m(Q_\epsilon)$ which have the properties

$$\langle F_i^n | F_j^m \rangle = \delta_{ij}\delta_{nm} \ ,$$

$$\langle F_i^n | Q_i | F_j^m \rangle = \delta_{ij} \times \begin{cases} (1/\alpha)[\tfrac{1}{2}(n+1)]^{1/2}, & m = n+1 \\ (1/\alpha)(\tfrac{1}{2}n)^{1/2}, & m = n-1 \\ 0 \ , & \text{otherwise} \ , \end{cases} \tag{3}$$

$$H_{\text{vib}} F_\theta^n F_\epsilon^m = \hbar\omega_e(n + m + 1) F_\theta^n F_\epsilon^m$$

[α is defined as $\alpha = (\mu\omega_e/\hbar)^{1/2}$]. The vibrational wave functions with 0, 1, and 2 phonons are given in Table I with their irreducible representations. The one-phonon functions $F_\theta^1 F_\epsilon^0$ and $F_\theta^0 F_\epsilon^1$ transform respectively as $\Gamma_{3\theta}$ and $\Gamma_{3\epsilon}$; the two-phonon wave functions are obtained from the product $\Gamma_3 \times \Gamma_3 = \Gamma_1 + \Gamma_2 + \Gamma_3$, using the tables of Koster *et al.*[10] We limited our calculations to the two-phonon functions.

C. Unperturbed vibronic energy levels

These are the eigenstates of

$$H_0 = H_{\mathrm{so}} + H_{\mathrm{vib}} \ ,$$

i.e., the wave functions are products of the spin-orbit and the vibrational functions given in Table I, whereas the energies are the sum of their energies. Using the tables of Koster *et al.* we obtained these vibronic functions and their transformation properties. There are 10 zero-phonon, 20 one-phonon, and 30 two-phonon vibronic functions. Table II gives, for example, the 0, 1, and 2-phonon vibronic functions which transform as Γ_1, Γ_{4z}, and $\Gamma_{5\zeta}$. Figure 1 represents the first two sets of unperturbed vibronic levels corresponding, respectively, to zero and one phonon levels which are deducible one from another by the constant energy shift $\hbar\omega_e = 70$ cm^{-1}.

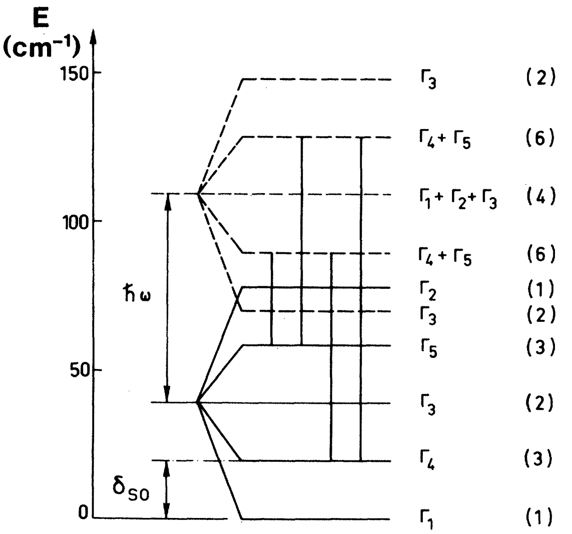

FIG. 1. Unperturbed vibronic energy levels originating from the ^5E state of Fe^{2+} in ZnS before modification by the Jahn-Teller Hamiltonian H_{JT}. Full line levels are zero phonon levels, dashed line levels are one phonon levels. Corresponding irreducible representations and degeneracies are given. The Jahn-Teller coupling between the Γ_4 levels and between the Γ_5 levels is schematized by vertical lines.

TABLE II. Unperturbed vibronic wave functions with zero, one, or two phonons for the representations Γ_1, Γ_{4z} and $\Gamma_{5\zeta}$, with the corresponding energies and the values of $\langle U_\theta \rangle$ and $\langle U_\epsilon \rangle$.

Unperturbed vibronic wave functions	Energy	$\langle U_\theta \rangle$	$\langle U_\epsilon \rangle$
$\lvert\Gamma_1\rangle_0 = \Gamma_1 F_\theta^0 F_\epsilon^0$	0	0	0
$\lvert\Gamma_1\rangle_1 = (1/\sqrt{2})(\Gamma_{3\theta} F_\theta^1 F_\epsilon^0 + \Gamma_{3\epsilon} F_\theta^0 F_\epsilon^1)$	$2\delta_{\mathrm{so}} + \hbar\omega_e$	0	0
$\lvert\Gamma_1\rangle_2 = \Gamma_1 (1/\sqrt{2})(F_\theta^2 F_\epsilon^0 + F_\theta^0 F_\epsilon^2)$	$2\hbar\omega_e$	0	0
$\lvert\Gamma_1\rangle_{2'} = (1/2)\Gamma_{3\theta}(-F_\theta^2 F_\epsilon^0 + F_\theta^0 F_\epsilon^2) + (1/\sqrt{2})\Gamma_{3\epsilon} F_\theta^1 F_\epsilon^1$	$2\delta_{\mathrm{so}} + 2\hbar\omega_e$	0	0
$\lvert\Gamma_{4z}\rangle_0 = \Gamma_{4z} F_\theta^0 F_\epsilon^0$	δ_{so}	1	0
$\lvert\Gamma_{4z}\rangle_1 = \Gamma_{4z} F_\theta^1 F_\epsilon^0$	$\delta_{\mathrm{so}} + \hbar\omega_e$	1	0
$\lvert\Gamma_{4z}\rangle_{1'} = \Gamma_{5\zeta} F_\theta^0 F_\epsilon^1$	$3\delta_{\mathrm{so}} + \hbar\omega_e$	-1	0
$\lvert\Gamma_{4z}\rangle_2 = \Gamma_{4z}(1/\sqrt{2})(F_\theta^2 F_\epsilon^0 + F_\theta^0 F_\epsilon^2)$	$\delta_{\mathrm{so}} + 2\hbar\omega_e$	1	0
$\lvert\Gamma_{4z}\rangle_{2'} = \Gamma_{4z}(1/\sqrt{2})(-F_\theta^2 F_\epsilon^0 + F_\theta^0 F_\epsilon^2)$	$\delta_{\mathrm{so}} + 2\hbar\omega_e$	1	0
$\lvert\Gamma_{4z}\rangle_{2''} = \Gamma_{5\zeta} F_\theta^1 F_\epsilon^1$	$3\delta_{\mathrm{so}} + 2\hbar\omega_e$	-1	0
$\lvert\Gamma_{5\zeta}\rangle_0 = \Gamma_{5\zeta} F_\theta^0 F_\epsilon^0$	$3\delta_{\mathrm{so}}$	-1	0
$\lvert\Gamma_{5\zeta}\rangle_1 = \Gamma_{4z} F_\theta^0 F_\epsilon^1$	$\delta_{\mathrm{so}} + \hbar\omega_e$	1	0
$\lvert\Gamma_{5\zeta}\rangle_{1'} = \Gamma_{5\zeta} F_\theta^1 F_\epsilon^0$	$3\delta_{\mathrm{so}} + \hbar\omega_e$	-1	0
$\lvert\Gamma_{5\zeta}\rangle_2 = \Gamma_{4z} F_\theta^1 f_\epsilon^1$	$\delta_{\mathrm{so}} + 2\hbar\omega_e$	1	0
$\lvert\Gamma_{5\zeta}\rangle_{2'} = \Gamma_{5\zeta}(1/\sqrt{2})(F_\theta^2 F_\epsilon^0 + F_\theta^0 F_\epsilon^2)$	$3\delta_{\mathrm{so}} + 2\hbar\omega_e$	-1	0
$\lvert\Gamma_{5\zeta}\rangle_{2''} = \Gamma_{5\zeta}(1/\sqrt{2})(-F_\theta^2 F_\epsilon^0 + F_\theta^0 F_\epsilon^2)$	$3\delta_{\mathrm{so}} + 2\hbar\omega_e$	-1	0

D. Jahn-Teller coupling

Taking into account the Jahn-Teller coupling, the Hamiltonian of the system becomes

$$H = H_{\text{so}} + H_{\text{vib}} + H_{\text{JT}} \ , \tag{4}$$

where the Jahn-Teller coupling in its linear form is

$$H_{\text{JT}} = V(Q_\theta U_\theta + Q_\epsilon U_\epsilon) \ . \tag{5}$$

The orbital operators U_θ and U_ϵ, which transform as $\Gamma_{3\theta}$ and $\Gamma_{3\epsilon}$ under T_d, are represented by the matrices

$$U_\theta = \begin{pmatrix} -1 & 0 \\ 0 & 1 \end{pmatrix}, \quad U_\epsilon = \begin{pmatrix} 0 & 1 \\ 1 & 0 \end{pmatrix}$$

with respect to the orbital electronic states ψ_θ, ψ_ϵ. The matrix elements of U_θ and U_ϵ within the spin-orbit functions of Table I are given in Table III.

According to group theory, H_{JT}, which is invariant under the full point-group symmetry, only couples those vibronic wave functions which belong to the same row of the same irreducible representation. The problem of determining the eigenstates of H thus consists in diagonalizing the corresponding submatrices. The submatrices of H for Γ_1, Γ_{4z}, and $\Gamma_{5\zeta}$ are given in Table IV. The matrices for Γ_{4x} and Γ_{4y} are similar to the matrix for Γ_{4z}, and the matrices for $\Gamma_{5\xi}$ and $\Gamma_{5\eta}$ to the matrix for $\Gamma_{5\zeta}$.

The solution was obtained by using a computer. The Jahn-Teller coupling not only shifts the energies of the zero-phonon vibronic levels, but also modifies their wave functions by admixing one- or two-

TABLE III. Matrices of U_θ and U_ϵ within the pure electronic spin-orbit wave functions of Table I.

U_θ

	Γ_1	Γ_2	$\Gamma_{3\theta}$	$\Gamma_{3\epsilon}$	Γ_{4x}	Γ_{4y}	Γ_{4z}	$\Gamma_{5\xi}$	$\Gamma_{5\eta}$	$\Gamma_{5\zeta}$
Γ_1			1							
Γ_2				-1						
$\Gamma_{3\theta}$	1									
$\Gamma_{3\epsilon}$		-1								
Γ_{4x}					$-\frac{1}{2}$			$-\frac{\sqrt{3}}{2}$		
Γ_{4y}						$-\frac{1}{2}$			$\frac{\sqrt{3}}{2}$	
Γ_{4z}							1			
$\Gamma_{5\xi}$					$-\frac{\sqrt{3}}{2}$			$\frac{1}{2}$		
$\Gamma_{5\eta}$						$\frac{\sqrt{3}}{2}$			$\frac{1}{2}$	
$\Gamma_{5\zeta}$										-1

U_ϵ

	Γ_1	Γ_2	$\Gamma_{3\theta}$	$\Gamma_{3\epsilon}$	Γ_{4x}	Γ_{4y}	Γ_{4z}	$\Gamma_{5\xi}$	$\Gamma_{5\eta}$	$\Gamma_{5\zeta}$
Γ_1				1						
Γ_2			1							
$\Gamma_{3\theta}$		1								
$\Gamma_{3\epsilon}$	1									
Γ_{4x}					$\frac{\sqrt{3}}{2}$			$-\frac{1}{2}$		
Γ_{4y}						$-\frac{\sqrt{3}}{2}$			$-\frac{1}{2}$	
Γ_{4z}										1
$\Gamma_{5\xi}$					$-\frac{1}{2}$			$-\frac{\sqrt{3}}{2}$		
$\Gamma_{5\eta}$						$-\frac{1}{2}$			$\frac{\sqrt{3}}{2}$	
$\Gamma_{5\zeta}$							1			

TABLE IV. Matrix elements of the Hamiltonian $H = H_{\rm so} + H_{\rm vib} + H_{\rm JT}$ within the vibronic wave functions of Table II, for the representations Γ_1, Γ_{4z}, and $\Gamma_{5\zeta}$.

	Γ_1			
	$\lvert\Gamma_1\rangle_0$	$\lvert\Gamma_1\rangle_1$	$\lvert\Gamma_1\rangle_2$	$\lvert\Gamma_1\rangle_{2'}$
$\lvert\Gamma_1\rangle_0$		V/α		
$\lvert\Gamma_1\rangle_1$	V/α	$2\delta_{\rm so}+\hbar\omega_e$	V/α	
$\lvert\Gamma_1\rangle_2$		V/α	$2\hbar\omega_e$	
$\lvert\Gamma_1\rangle_{2'}$				$2\delta_{\rm so}+2\hbar\omega_e$

	Γ_{4z}					
	$\lvert\Gamma_{4z}\rangle_0$	$\lvert\Gamma_{4z}\rangle_1$	$\lvert\Gamma_{4z}\rangle_{1'}$	$\lvert\Gamma_{4z}\rangle_2$	$\lvert\Gamma_{4z}\rangle_{2'}$	$\lvert\Gamma_{4z}\rangle_{2''}$
$\lvert\Gamma_{4z}\rangle_0$	$\delta_{\rm so}$	$V/\alpha\sqrt{2}$	$V/\alpha\sqrt{2}$			
$\lvert\Gamma_{4z}\rangle_1$	$V/\alpha\sqrt{2}$	$\delta_{\rm so}+\hbar\omega_e$		$V/\alpha\sqrt{2}$	$-V/\alpha\sqrt{2}$	$V/\alpha\sqrt{2}$
$\lvert\Gamma_{4z}\rangle_{1'}$	$V/\alpha\sqrt{2}$		$3\delta_{\rm so}+\hbar\omega_e$	$V/\alpha\sqrt{2}$	$V/\alpha\sqrt{2}$	$-V/\alpha\sqrt{2}$
$\lvert\Gamma_{4z}\rangle_2$		$V/\alpha\sqrt{2}$	$V/\alpha\sqrt{2}$	$\delta_{\rm so}+2\hbar\omega_e$		
$\lvert\Gamma_{4z}\rangle_{2'}$		$-V/\alpha\sqrt{2}$	$V/\alpha\sqrt{2}$		$\delta_{\rm so}+2\hbar\omega_e$	
$\lvert\Gamma_{4z}\rangle_{2''}$		$V/\alpha\sqrt{2}$	$-V/\alpha\sqrt{2}$			$3\delta_{\rm so}+2\hbar\omega_e$

	$\Gamma_{5\zeta}$					
	$\lvert\Gamma_{5\zeta}\rangle_0$	$\lvert\Gamma_{5\zeta}\rangle_1$	$\lvert\Gamma_{5\zeta}\rangle_{1'}$	$\lvert\Gamma_{5\zeta}\rangle_2$	$\lvert\Gamma_{5\zeta}\rangle_{2'}$	$\lvert\Gamma_{5\zeta}\rangle_{2''}$
$\lvert\Gamma_{5\zeta}\rangle_0$	$3\delta_{\rm so}$	$V/\alpha\sqrt{2}$	$-V/\alpha\sqrt{2}$			
$\lvert\Gamma_{5\zeta}\rangle_1$	$V/\alpha\sqrt{2}$	$\delta_{\rm so}+\hbar\omega_e$		$V/\alpha\sqrt{2}$	$V/\alpha\sqrt{2}$	$V/\alpha\sqrt{2}$
$\lvert\Gamma_{5\zeta}\rangle_{1'}$	$-V/\alpha\sqrt{2}$		$3\delta_{\rm so}+\hbar\omega_e$	$V/\alpha\sqrt{2}$	$-V/\alpha\sqrt{2}$	$V/\alpha\sqrt{2}$
$\lvert\Gamma_{5\zeta}\rangle_2$		$V/\alpha\sqrt{2}$	$V/\alpha\sqrt{2}$	$\delta_{\rm so}+2\hbar\omega_e$		
$\lvert\Gamma_{5\zeta}\rangle_{2'}$		$V/\alpha\sqrt{2}$	$-V/\alpha\sqrt{2}$		$3\delta_{\rm so}+2\hbar\omega_e$	
$\lvert\Gamma_{5\zeta}\rangle_{2''}$		$V/\alpha\sqrt{2}$	$V/\alpha\sqrt{2}$			$3\delta_{\rm so}+2\hbar\omega_e$

phonon functions. This then changes the quadrupole interaction associated with the triplets Γ_4 and Γ_5.

E. Quadrupole interaction

The quadrupole Hamiltonian is[4]

$$H_Q = C_E\{U_\theta[3I_z^2 - I(I+1)] + U_\epsilon\sqrt{3}(I_x^2 - I_y^2)\} \ , \quad (6)$$

with

$$C_E = \tfrac{1}{7}\langle r^{-3}\rangle \frac{e^2Q}{I(2I-1)} \ (I = \tfrac{3}{2} \text{ for } ^{57}\text{Fe, 14.4 keV}) \ .$$

Triplet Γ_4. Even in good samples having a low defect level the degeneracy of the zero-phonon Γ_4 triplet is removed by random strains which slightly separate the states Γ_{4x}, Γ_{4y}, and Γ_{4z} from each other.

In the absence of Jahn-Teller coupling the three corresponding wave functions are the unperturbed $\lvert\Gamma_{4x}\rangle_0$, $\lvert\Gamma_{4y}\rangle_0$, and $\lvert\Gamma_{4z}\rangle_0$ vibronic wave functions whose electronic parts are respectively Γ_{4x}, Γ_{4y}, and Γ_{4z}. Using the matrix elements of U_θ and U_ϵ listed in Table III, the quadrupole separation given by Eq. (6) is found to be the same for the three sublevels. The common value is easily calculated in the sublevel $\lvert\Gamma_{4z}\rangle_0$ where $\langle U_\theta\rangle = +1$ and $\langle U_\epsilon\rangle = 0$ (Table II), and it is equal to

$$(\Delta E_Q)_0 = 6\lvert C_E\rvert \ . \quad (7)$$

In the presence of Jahn-Teller coupling the actual vibronic wave functions of the Γ_4 triplet result from one- and two-phonon admixtures, following the expression

$$\lvert\Gamma_{4i}\rangle = a\lvert\Gamma_{4i}\rangle_0 + b\lvert\Gamma_{4i}\rangle_1 + b'\lvert\Gamma_{4i}\rangle_{1'} + c\lvert\Gamma_{4i}\rangle_2 + c'\lvert\Gamma_{4i}\rangle_{2'} + c''\lvert\Gamma_{4i}\rangle_{2''} \quad (8)$$

$$(i = x,y,z) \ ,$$

where a,b,b',c,c',c'' are real coefficients satisfying the normalization condition

$$a^2 + b^2 + b'^2 + c^2 + c'^2 + c''^2 = 1 \ . \quad (9)$$

The quadrupole splitting again has the same value for the three sublevels labeled by $i=x,y,z$, but this value $\Delta E_Q(\Gamma_4)$ is reduced compared to $(\Delta E_Q)_0$ in Eq. (7):

$$\Delta E_Q(\Gamma_4)=q(\Gamma_4)6|C_E| \ . \tag{10}$$

The reduction coefficient $q(\Gamma_4)$ is easily calculated for the wave function $|\Gamma_{4z}\rangle$. Using Eqs. (8) and (9) and the expectation values $\langle U_\theta\rangle$ and $\langle U_\epsilon\rangle$ given in Table II, we find

$$\begin{aligned} q(\Gamma_4) &= |\langle\Gamma_{4z}|U_\theta|\Gamma_{4z}\rangle| \\ &= |a^2+b^2+c^2+c'^2-b'^2-c''^2| \end{aligned}$$

or

$$q(\Gamma_4)=|1-2(b'^2+c''^2)| \ . \tag{11}$$

Triplet Γ_5. In the same way the sublevels transforming as $\Gamma_{5\xi}$, $\Gamma_{5\eta}$, and $\Gamma_{5\zeta}$ are separated by the strains and they also give a common quadrupole splitting.

In the absence of Jahn-Teller coupling this quadrupole splitting is easily calculated in the $|\Gamma_{5\zeta}\rangle_0$ vibronic wave function where $\langle U_\theta\rangle=-1$ and $\langle U_\epsilon\rangle=0$ (Table II), and the result is again given by Eq. (7), although the sign of the electric field gradient is reversed compared to that of the corresponding Γ_4 sublevels.

In the presence of Jahn-Teller coupling the modified vibronic wave functions are

$$\begin{aligned} |\Gamma_{5j}\rangle &= A|\Gamma_{5j}\rangle_0 + B|\Gamma_{5j}\rangle_1 + B'|\Gamma_{5j}\rangle_{1'} \\ &\quad + C|\Gamma_{5j}\rangle_2 + C'|\Gamma_{5j}\rangle_{2'} + C''|\Gamma_{5j}\rangle_{2''} \\ &\qquad (j=\xi,\eta,\zeta) \ , \end{aligned} \tag{12}$$

with

$$A^2+B^2+B'^2+C^2+C'^2+C''^2=1 \ . \tag{13}$$

The quadrupole splitting is then

$$\Delta E_Q(\Gamma_5)=q(\Gamma_5)6|C_E| \tag{14}$$

with

$$\begin{aligned} q(\Gamma_5) &= |\langle\Gamma_{5\zeta}|U_\theta|\Gamma_{5\zeta}\rangle| \\ &= |B^2+C^2-A^2-B'^2-C'^2-C''^2| \end{aligned}$$

or

$$q(\Gamma_5)=|1-2(B^2+C^2)| \ . \tag{15}$$

It is worthwhile examining in a qualitative way the physical reason which leads to the result $q(\Gamma_5) < q(\Gamma_4)$. For this purpose we can neglect the two-phonon admixtures in the wave functions (8) and (12), and use for the reduction factors the simplified expressions $q(\Gamma_4)\simeq|1-2b'^2|$ and $q(\Gamma_5) \simeq |1-2B^2|$ instead of Eqs. (11) and (15). Figure 1 and Table II show that the level $|\Gamma_4\rangle_{1'}$ which is responsible for the mixing coefficient b', is distant from the level $|\Gamma_4\rangle_0$ by an energy shift $\hbar\omega_e+2\delta_{so} \sim 110$ cm^{-1}, whereas the level $|\Gamma_5\rangle_1$ which is responsible for the mixing coefficient B is distant from the level $|\Gamma_5\rangle_0$ by an energy shift $\hbar\omega_e-2\delta_{so}\sim 30$ cm^{-1}. As this latter value is much smaller than the former value, the perturbation of $|\Gamma_5\rangle_0$ by $|\Gamma_5\rangle_1$ is larger than the perturbation of $|\Gamma_4\rangle_0$ by $|\Gamma_4\rangle_{1'}$, which gives $B^2 > b'^2$ and $q(\Gamma_5) < q(\Gamma_4)$.

F. Fit to the experimental data

Only two parameters are considered as being adjustable in the problem: δ_{so}, the initial splitting of the unperturbed spin-orbit levels, which is connected by relation (1) to the spin-orbit parameter λ; and the Jahn-Teller energy $E_{JT}=V^2/(2\alpha^2\hbar\omega_e)$.

The requirements are that the calculated energies of the modified zero phonon levels Γ_4, Γ_3, and Γ_5 agree with the optically measured energies[2] $E(\Gamma_4) = 15.0$ cm^{-1}, $E(\Gamma_3)=27.5$ cm^{-1}, and $E(\Gamma_5) = 45.0$ cm^{-1}, and also that the calculated quadrupole reduction factors $q(\Gamma_4)$ and $q(\Gamma_5)$ agree with the experimental values $q(\Gamma_4)=0.917$ and $q(\Gamma_5)=0.40$.

By means of the vibronic calculation, these five experimental data give five different relations between the two adjustable parameters δ_{so} and E_{JT}. The best solution is graphically determined in a δ_{so}, E_{JT} plot from the intersection of the corresponding curves (Fig. 2). It appears that the three curves given by the data of the energy levels $E(\Gamma_4)$, $E(\Gamma_3)$, and $E(\Gamma_5)$ are very roughly parallel, so that their intersection is not well definite. This observation is related to the fact that both covalency and the Jahn-Teller effect participate in the reduction of the spin-orbit separation from the free ion value, and that the two effects cannot be separated as long as the departure from equidistance in the levels remains small. But the knowledge of the quadrupole reduction factor $q(\Gamma_5)$ introduces an independent and very restrictive condition on the vibronic wave functions $|\Gamma_{5j}\rangle$, which corresponds to a curve in a transverse direction (compared to the three previous curves) on the δ_{so}, E_{JT} plot. Although $q(\Gamma_4)$ also gives another transverse curve (dashed line curve, Fig. 2), this latter relation is less restrictive because $q(\Gamma_4)$ is closer to unity than $q(\Gamma_5)$ and much less sensitive to the δ_{so} and E_{JT} values. Taking this observation into account, the solution which optimizes the five experimental results is given by $\delta_{so}=19.5\pm0.5$ cm^{-1} and $E_{JT}=14\pm2$ cm^{-1}.

The corresponding mixing coefficients in the vibronic wave functions (8) and (12) of the levels Γ_4 and Γ_5 are given in Table VI.

Figure 3 shows the variation of the spin-orbit energy levels and of the quadrupole reduction factors $q(\Gamma_4)$ and $q(\Gamma_5)$ as a function of the Jahn-Teller en-

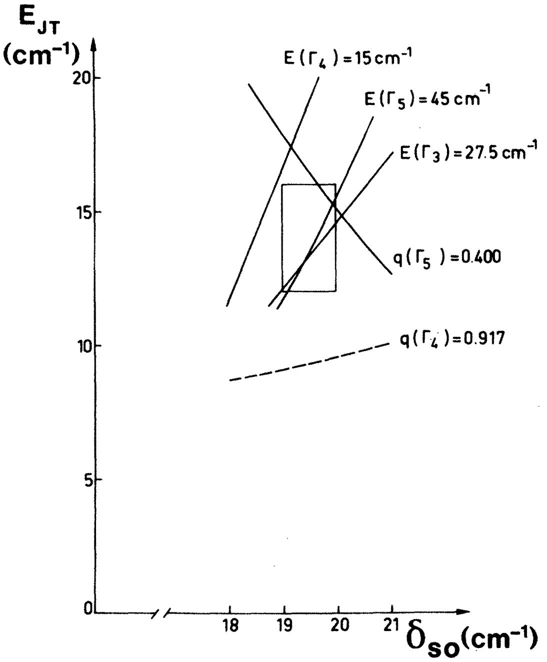

FIG. 2. Graphic determination of the parameters δ_{so} and E_{JT} in the vibronic calculation. The experimental values of the energy levels $E(\Gamma_3)$, $E(\Gamma_4)$, $E(\Gamma_5)$, and of the quadrupole reduction factors $q(\Gamma_4)$ and $q(\Gamma_5)$ yield 5 relation curves on the δ_{so}, E_{JT} plot. The values $\delta_{so} = 19.5 \pm 0.5$ cm^{-1} and $E_{JT} = 14 \pm 2$ cm^{-1} give the best agreement with the various experimental results.

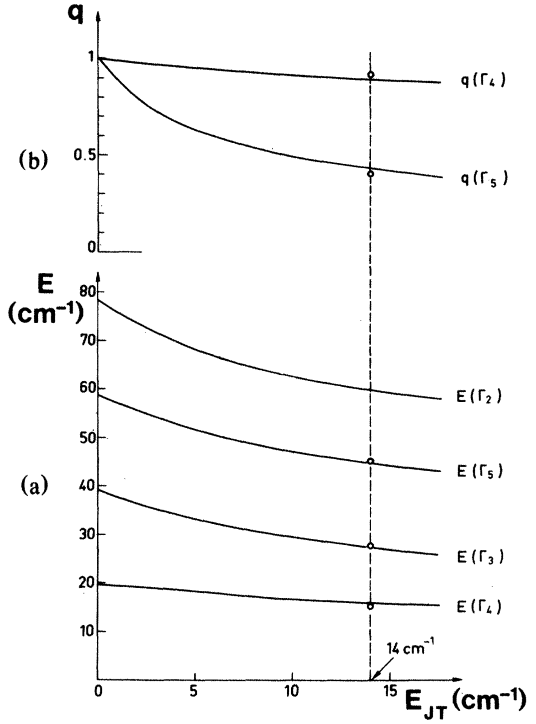

FIG. 3. (a) Variation of the spin-orbit energy levels Γ_4, Γ_3, Γ_5, Γ_2 as a function of the Jahn-Teller energy E_{JT} (ground state level Γ_1: zero energy). (b) Variation of the quadrupole reduction factors $q(\Gamma_4)$ and $q(\Gamma_5)$ vs E_{JT}. The initial spin-orbit separation is taken to be $\delta_{so} = 19.5$ cm^{-1} in the calculation. The best agreement with the experimental values (open circles) is obtained for $E_{JT} \sim 14$ cm^{-1}.

ergy E_{JT}, using the value $\delta_{so} = 19.5$ cm^{-1}. The values of these functions for $E_{JT} = 14$ cm^{-1} can be compared with the experimental values (see also Table V). The agreement is satisfactory, especially if we consider the various approximations inherent to the vibronic model.

Neglecting the fact that the spin-orbit levels are no longer equidistant when reduced by the Jahn-Teller coupling [Fig. 3(a)], a mean reduction factor $q \simeq 0.77$ is observed for the total spin-orbit splitting for $E_{JT} = 14$ cm^{-1}. This is not far from the value $q \simeq 0.72$ given by perturbation theory[4]:

$$q \simeq \frac{1}{2}\left[1 + \exp\left(-4\frac{E_{JT}}{\hbar\omega_e}\right)\right]$$

for $E_{JT} = 14$ cm^{-1} and $\hbar\omega_e = 70$ cm^{-1}, although the

TABLE V. Comparison between experimental data and calculated values. The values $\hbar\omega_e = 70$ cm^{-1} (phonon energy); $\delta_{so} = 19.5$ cm^{-1} (initial spin-orbit separation) and $E_{JT} = 14$ cm^{-1} (Jahn-Teller energy) were used in the calculation. $E(\Gamma_4)$, $E(\Gamma_3)$, $E(\Gamma_5)$ are, respectively, the energies of the levels Γ_4, Γ_3, Γ_5 and $q(\Gamma_4)$, $q(\Gamma_5)$ are the quadrupole reduction factors in Γ_4 and Γ_5.

	$E(\Gamma_4)$ (cm^{-1})	$E(\Gamma_3)$ (cm^{-1})	$E(\Gamma_5)$ (cm^{-1})	$q(\Gamma_4)$	$q(\Gamma_5)$
Calculated values	15.85	27.16	44.71	0.891	0.428
Experimental values	15.0[a]	27.5[a]	45.0[a]	0.917±0.02[b]	0.400±0.02[b]

[a] Reference 2.

[b] This work.

condition $\hbar\omega_e > 4\delta_{\text{so}}$ is not fulfilled here ($4\delta_{\text{so}} \simeq 78$ cm^{-1}).

The Jahn-Teller energy for the ^5E state of Fe^{2+} is found to be more important in ZnS ($E_{\text{JT}} \simeq 14$ cm^{-1}) than in CdTe [$E_{\text{JT}} \simeq 4.2$ cm^{-1} (Ref. 5)]. However the Jahn-Teller perturbation of the levels is less important in ZnS because the energy $\hbar\omega_e$ of the vibrational mode is about two times larger than in CdTe. Owing to the various approximations made in the calculation, the fitted value $E_{\text{JT}} \simeq 14$ cm^{-1} is only an approximate value. Amongst these approximations let us mention the use of a single effective vibrational mode $\hbar\omega_e = 70$ cm^{-1} in the Jahn-Teller coupling, the limitation of the calculation to the linear Jahn-Teller Hamiltonian excluding the "warping terms"[11,12] and the limitation to the zero, one, and two phonon vibronic wave functions. The present experimental determination of E_{JT} however shows that the value $E_{\text{JT}} \simeq 62$ cm^{-1} predicted by Natadze and Ryskin[13] for the ^5E state of Fe^{2+} in ZnS was overestimated.

The covalency effect on the spin-orbit parameter λ can be estimated from the relation (1). Using the values $p = +0.95$ cm^{-1}, $\Delta = 3400$ cm^{-1} and the fitted value $\delta_{\text{so}} = 19.5 \pm 0.5$ cm^{-1}, we find $\lambda = -88.4 \pm 1.6$ cm^{-1}. Compared to the free-ion value $\lambda_0 \simeq -100$ cm^{-1}, this value corresponds to a moderate covalency reduction, which is less important than for Fe^{2+} in CdTe [$\lambda \simeq -79$ cm^{-1} (Ref. 5)]. This observation agrees with the comparison of the cubic field splitting parameter Δ in the two systems: the parameter Δ, which is strongly covalency dependent, is again more reduced in CdTe ($\Delta = 2480$ cm^{-1}) than in ZnS ($\Delta = 3400$ cm^{-1}).[14]

IV. INFLUENCE OF STRAINS AND OF APPLIED MAGNETIC FIELDS

It is interesting to examine how the Fe^{2+} Mössbauer emission spectrum is modified when the ZnS sample is submitted to applied strains or to external magnetic fields. To obtain detailed information however such experiments would require the use of single crystals. Unfortunately good single crystals of ZnS in the cubic phase (blende) are particularly difficult to obtain, and for the crystals at our disposal the intrinsic strain level was too high to allow such experiments being made. Although only polycrystalline experimental data are available at this time, it is worth while examining briefly some predictions of the vibronic calculation in the presence of large strains or applied magnetic fields.

A. Strain effects

We consider here how the quadrupole interaction in the vibronic levels Γ_1, Γ_4, and Γ_5 is modified by strains when the strain separations are not small compared to the spin-orbit splitting. The general strain Hamiltonian acting within the orbital ^5E doublet has the form[11]

$$H_S = E_\theta U_\theta + E_\epsilon U_\epsilon \ .$$

The total Hamiltonian of the system is now

$$H = H_{\text{so}} + H_{\text{vib}} + H_S + H_{\text{JT}} \ .$$

This Hamiltonian acts separately within the following groups of representations: $\Gamma_1 + \Gamma_2 + \Gamma_3$; $\Gamma_{4x} + \Gamma_{5\xi}$; $\Gamma_{4y} + \Gamma_{5\eta}$; $\Gamma_{4z} + \Gamma_{5\zeta}$, which gives one matrix 24×24 and three matrices 12×12 to be diagonalized within the 0, 1, and 2 phonon vibronic wave functions. The quadrupole interaction is then calculated within the strain modified wave functions. Let $q(\Gamma_1)$, $q(\Gamma_{4i})$, and $q(\Gamma_{5j})$ be the reduced quadrupole splittings in the vibronic levels Γ_1, Γ_{4i}, and Γ_{5j}, i.e., the actual quadrupole splittings are these reduced quantities multiplied by the factor $6|C_E| \simeq 3.27$ mm s^{-1}. Using the same values $E_{\text{JT}} = 14$ cm^{-1} and $\delta_{\text{so}} = 19.5$ cm^{-1} as in Sec. III, we computed the values of the reduced quadrupole splittings as a function of the strain intensity for two particular deformation symmetries: E_θ variable with $E_\epsilon = 0$ (tetragonal distortion along Oz) and E_ϵ variable with $E_\theta = 0$ (orthorhombic distortion in Oxy). The results are shown in Fig. 4. As expected, vanishing strains give a vanishing quadrupole interaction $q(\Gamma_1)$ in the ground singlet Γ_1, while the 3 values $q(\Gamma_{4x,y,z})$ tend to the same finite value $q(\Gamma_4) \simeq 0.891$ and $q(\Gamma_{5\xi,\eta,\zeta})$ tend to the finite value $q(\Gamma_5) \simeq 0.428$. For low strain intensity, whatever the symmetry of the strain, the separation between the $q(\Gamma_{5\xi,\eta,\zeta})$ values is about eight times larger than the corresponding separation between the $q(\Gamma_{4x,y,z})$ values; therefore the strain broadening of the lines in the emission Mössbauer spectra should be eight times larger for the internal doublet than for the external doublet. Experimentally however the difference seems to be somewhat smaller than predicted.

B. Applied magnetic fields

The Zeeman Hamiltonian $H_Z = \mu_B \vec{H} \cdot (\vec{L} + 2\vec{S})$ in the ^5E state of Fe^{2+} may be expressed as

$$H_Z = g_1 \mu_B (\vec{S} \cdot \vec{H}) + \tfrac{1}{2} g_2 \mu_B \{[3S_z H_z - (\vec{S} \cdot \vec{H})] U_\theta + \sqrt{3}(S_x H_x - S_y H_y) U_\epsilon\} \ , \tag{16}$$

where g_1 and g_2 are given by

$$g_1 = 2 - (4\lambda/\Delta); \quad g_2 = -(4\lambda/\Delta) \tag{17}$$

to first-order perturbation in the spin-orbit interaction between ^5E and $^5T_2$.[2,5,11,15]

The matrix elements of Eq. (16) within the spin-

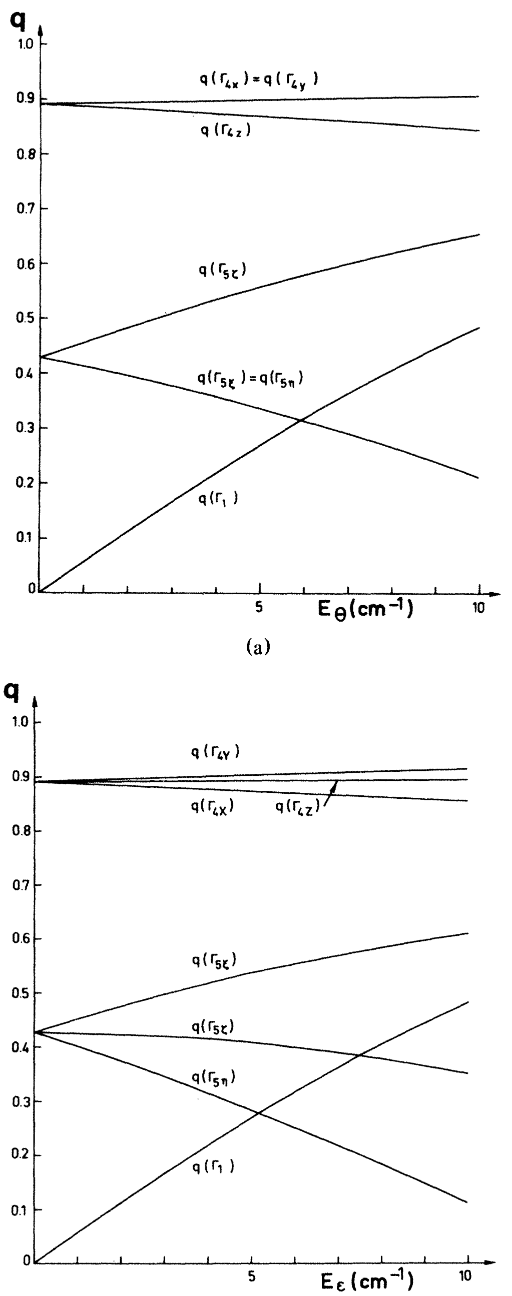

(a)

(b)

FIG. 4. Reduced quadrupole interactions $q(\Gamma_1)$, $q(\Gamma_{4x,y,z})$, $q(\Gamma_{5\xi,\eta,\zeta})$ calculated as a function of the strain parameters, (a): vs E_θ (with $E_\epsilon=0$); (b): vs E_ϵ (with $E_\theta=0$).

orbit functions of Table I are given in Table III of Ref. 2.

As long as the Zeeman splittings of the vibronic triplets Γ_4 and Γ_5 are small compared to the spin-orbit separation, we can evaluate the g factors in these triplets by equating the matrix elements of Eq. (16) within the vibronic wave functions $|\Gamma_{4i}\rangle$ Eq. (8) and $|\Gamma_{5j}\rangle$ Eq. (12), with the matrix elements of the respective Hamiltonians

$$H_Z(\Gamma_4)=g(\Gamma_4)\mu_B(\vec{J}\cdot\vec{H}) \ , \tag{18}$$

$$H_Z(\Gamma_5)=g(\Gamma_5)\mu_B(\vec{J}'\cdot\vec{H}) \ , \tag{19}$$

which are expressed in terms of the effective spins $J=1$ and $J'=1$.

We obtained the results:

$$\begin{aligned} g(\Gamma_4)={}&\left(1+\frac{2\lambda}{\Delta}\right)\left(a^2+c^2-\frac{b^2}{2}-\frac{c'^2}{2}\right)\\ &-\tfrac{1}{2}\left(1-\frac{6\lambda}{\Delta}\right)(b'^2+c''^2)\\ &+3\left(1-\frac{2\lambda}{\Delta}\right)(bb'+c'c'') \ , \end{aligned} \tag{20}$$

$$\begin{aligned} g(\Gamma_5)={}&\left(1-\frac{6\lambda}{\Delta}\right)\left(A^2+C'^2-\frac{B'^2}{2}-\frac{C''^2}{2}\right)\\ &-\tfrac{1}{2}\left(1+\frac{2\lambda}{\Delta}\right)(B^2+C^2)\\ &-3\left(1-\frac{2\lambda}{\Delta}\right)(BB'+CC'') \ . \end{aligned} \tag{21}$$

[The relation (20) is to be compared to the relation (24) of Vallin.[5]]

With $\lambda=-88.4$ cm^{-1} (Sec. III), $\Delta=3400$ cm^{-1} and the coefficient values $a,b,c,\ldots,$ and $A,B,C,\ldots,$ as given in Table VI, we found

$$g(\Gamma_4)\simeq 0.94, \quad g(\Gamma_5)\simeq 0.99 \ . \tag{22}$$

[With the λ/Δ terms but without the Jahn-Teller coupling the g factors are $g(\Gamma_4)\simeq 0.95$ and $g(\Gamma_5)\simeq 1.16$. Alternatively, with Jahn-Teller coupling but without the λ/Δ terms, we find $g(\Gamma_4)\simeq 0.97$ and $g(\Gamma_5)\simeq 0.86$. Finally $g(\Gamma_4)$ and $g(\Gamma_5)$ are obviously equal to 1 when both the Jahn-Teller effect and λ/Δ are neglected.]

One notices first that the Jahn-Teller reduction in the g factors is much less important than the corresponding reduction in the quadrupole interaction (Sec. III). Although the Jahn-Teller reduction in $g(\Gamma_5)$ is larger than in $g(\Gamma_4)$, this effect cannot compensate for the initial difference due to the factor λ/Δ, and the net value of the g factor is still a little larger in Γ_5 than in Γ_4.

These results are to be compared to the far infrared study of ZnS:Fe^{2+} in applied magnetic fields made by Vallin *et al.*[2] The variation of the energy levels with magnetic induction along the [001] and [101] directions, which were calculated by these authors using $\lambda=-73$ cm^{-1}, $\Delta=3400$ cm^{-1} and neglecting the Jahn-Teller effect (Figs. 6 and 7 and

TABLE VI. Mixing coefficients in the vibronic wave functions $|\Gamma_{4i}\rangle$ $(i=x,y,z)$, $|\Gamma_{5j}\rangle$ $(j=\xi,\eta,\zeta)$ and Γ_1 (relations 8, 12, and 25) resulting from the Jahn-Teller coupling. The calculation was made using the values $\delta_{so}=19.5$ cm^{-1} and $E_{JT}=14$ cm^{-1}.

Vibronic wave function	Coefficient values					
$\lvert\Gamma_1\rangle$	$\alpha=0.927$;	$\beta=-0.361$;	$\gamma=0.102$;	$\gamma'=0.000$		
$\lvert\Gamma_{4i}\rangle$	$a=0.894$;	$b=-0.364$;	$b'=-0.232$;	$c=0.116$;	$c'=-0.026$;	$c''=0.021$
$\lvert\Gamma_{5j}\rangle$	$A=0.792$;	$B=-0.531$;	$B'=0.254$;	$C=0.066$;	$C'=0.144$;	$C''=0.051$

Table III of Ref. 2), correspond to the values $g(\Gamma_4)\simeq 0.96$ and $g(\Gamma_5)\simeq 1.13$ in the low-field region. Taking into account the precision of the experimental points in these figures, it seems clear that the values $g(\Gamma_4)\simeq 0.94$ and $g(\Gamma_5)\simeq 0.99$ resulting from our vibronic calculation are also compatible with the experimental data.

The predictions concerning the effect of a magnetic field on the low-temperature emission Mössbauer spectra are as follows. The magnetic field, applied along any direction Om, is supposed to be strong enough to overcome the strain effects, without however leading to appreciable mixing between the spin-orbit levels (a situation which is hardly realized experimentally because the initial strain splittings usually reach 1 or 2 cm^{-1} in actual samples). With this assumption the magnetic sublevels of Γ_4 and Γ_5 which correspond to the effective spin components J_m and $J_{m'}=\pm 1$ in relations (18) and (19), induce isotropic hyperfine fields on the nucleus, which are alternatively increased or decreased by the amount of the external magnetic field. On the other hand the hyperfine field is zero in the diamagnetic sublevels $J_m=0$ and $J_{m'}=0$, as well as in the ground-state singlet Γ_1, so that the effective field on the nucleus reduces to the external magnetic field in these levels. It is easy to demonstrate that the principal axes of the electric field gradient (EFG) in the various sublevels of Γ_4 and Γ_5 remain the crystallographic axes Ox, Oy, and Oz whatever the direction Om of the magnetic field, but these EFG are generally no longer axially symmetric. Moreover the EFG in the magnetic sublevels $J_m=\pm 1$ and $J_{m'}=\pm 1$ are, respectively, equal to the EFG in the diamagnetic sublevels $J_m=0$ and $J_{m'}=0$ multiplied by the factor $-\frac{1}{2}$. The EFG remains zero in the level Γ_1.

Two particular cases are discussed hereafter.

1. Magnetic field applied along the [111] direction

The quadrupole interaction should vanish for symmetry reasons in all the sublevels of Γ_4 and Γ_5, and the slow relaxation emission spectrum should consist of the superimposition of 7 symmetrical Zeeman pattern originating from the 6 sublevels of Γ_4 and Γ_5 and from the level Γ_1. If the magnetic field is parallel to the γ ray propagation direction each if these Zeeman pattern would display only four lines because of the absence of the $\Delta m=0$ transitions.

2. Magnetic field applied along the [001] direction ($Om \parallel Oz$)

The EFG are axially symmetric along Oz, with opposite signs in the corresponding sublevels of the two triplets Γ_4 and Γ_5. The diamagnetic sublevels $J_m=0$ and $J_{m'}=0$ are the states $|\Gamma_{4z}\rangle$ and $|\Gamma_{5\zeta}\rangle$ which are already eigenstates in the absence of external field, and whose quadrupole interactions are given in relations (10), (11), (14), and (15). Due to the quadrupole interactions the Zeeman patterns coming from the sublevels of Γ_4 and Γ_5 are no longer symmetrical.

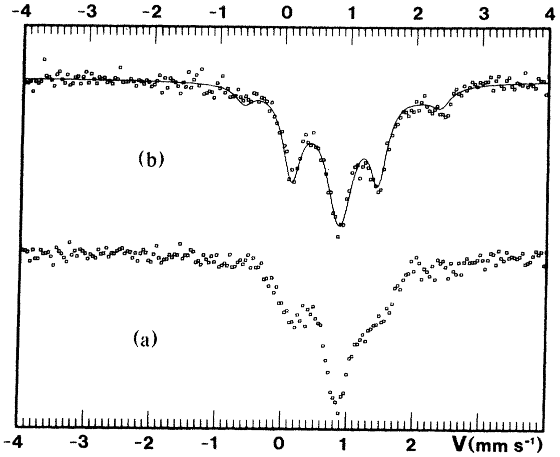

FIG. 5. Emission Mössbauer spectra of a ZnS: ^{57}Co powder sample at 1.3 K: (a) in an applied magnetic field $H=1$ T parallel to the γ rays; and (b) with $H=0$. The figure shows how the two quadrupole doublets due to the levels Γ_4 and Γ_5 are smoothed out by a moderate external field which overcome the strain splittings of these levels.

The $\Delta m = 0$ transitions again would disappear when the magnetic field is parallel to the γ ray direction.

Theoretical emission spectra can be easily simulated in these two particular cases, and they could be compared to single-crystal data if available.

Powder emission spectra in applied magnetic fields (Fig. 5) are of lesser interest as they consist of a very broad lineshape resulting from the superimposition of spectra corresponding to different relative orientations of the field within the crystal axes. They qualitatively verify however that the two quadrupole doublets assigned to the levels Γ_4 and Γ_5 are considerably modified by the magnetic hyperfine interaction as soon as the magnetic interaction on these levels becomes comparable to their initial strain splitting. The strain splitting, as deduced from the central line width data, was typically 2 cm^{-1} in our sample, and the quadrupole doublets are actually considerably smoothed in a magnetic field of 1 T [Fig. 5(a)] which corresponds to theoretical magnetic splittings of about 1 cm^{-1} in Γ_4 and Γ_5.

V. ISOMER SHIFT

As already mentioned (Part I, Sec. V B) the fitted isomer shift values of the three Fe^{2+} components in the emission spectra are not identical. The values at 1.3 K, compared to $\mathrm{K_4Fe(CN)_6 \cdot 3H_2O}$ at room temperature are, respectively:

$$S(\Gamma_1) = 0.84 \pm 0.01 \text{ mm s}^{-1} \quad \text{(central line)},$$
$$S(\Gamma_4) = 0.83 \pm 0.01 \text{ mm s}^{-1} \quad \text{(external quadrupole doublet)},$$
$$S(\Gamma_5) = 0.77 \pm 0.01 \text{ mm s}^{-1} \quad \text{(internal quadrupole doublet)}.$$

Whereas the first two values are comparable to the isomer shift value of the single line in the absorption experiments below 4.2 K ($S = 0.83 \pm 0.01$ mm s^{-1}), the third value is definitely smaller.

Such a difference seemed at first incompatible with the assignment of the corresponding quadrupole doublet to the Γ_5 level, as the various spin-orbit levels were thought *a priori* to give the same isomer shift.[7] This effect however could be qualitatively explained once the vibronic properties of the various spin-orbit levels were known.[9] The apparent or total isomer shift value comprises two terms: the chemical isomer shift and the second-order Doppler shift. The former term originates from the electronic density at the nucleus and probably does not vary from one spin-orbit level to another. But the latter term is correlated to the vibrational properties of the emitting nucleus, and it is supposed to depend on the vibronic properties of each level.

The second order Doppler shift D ($\mathrm{cm\,s}^{-1}$) is given by[16]

$$\frac{D}{c_0} = \frac{\delta E}{E} = -\frac{E_c}{mc_0^2} , \tag{23}$$

where E_c is the kinetic energy of the emitting nucleus, m the mass of this nucleus, and c_0 the light velocity.

Increasing vibrational zero point motion of the Mössbauer atom induces a decreasing D value and therefore a decreasing total isomer-shift value. The lowest isomer shift value of the Γ_5 contribution can thus be related to the largest vibrational energy in this level. Admitting that E_c is proportional to the fraction of one (or two) phonon wave function which is admixed into the zero phonon wave function in the various vibronic levels, we obtain the following relations between the second-order Doppler shifts $D(\Gamma_1)$, $D(\Gamma_4)$, and $D(\Gamma_5)$,

$$\frac{D(\Gamma_1)}{\beta^2 + 2(\gamma^2 + \gamma'^2)} = \frac{D(\Gamma_4)}{b^2 + b'^2 + 2(c^2 + c'^2 + c''^2)} = \frac{D(\Gamma_5)}{B^2 + B'^2 + 2(C^2 + C'^2 + C''^2)} , \tag{24}$$

where the coefficients β, γ, and γ' are those of the wave function

$$|\Gamma_1\rangle = \alpha|\Gamma_1\rangle_0 + \beta|\Gamma_1\rangle_1 + \gamma|\Gamma_1\rangle_2 + \gamma'|\Gamma_1\rangle_{2'} \tag{25}$$

(with $\alpha^2 + \beta^2 + \gamma^2 + \gamma'^2 = 1$), and where the coefficients b, b', c, c', c'' for $|\Gamma_4\rangle$ and B, B', C, C', C'' for $|\Gamma_5\rangle$ are defined in relations (8) and (12). Using the calculated values of these coefficients (Table VI), the relation (24) gives

$$D(\Gamma_1) - D(\Gamma_4) = 0.26[D(\Gamma_1) - D(\Gamma_5)] ,$$
$$S(\Gamma_1) - S(\Gamma_4) = 0.26[S(\Gamma_1) - S(\Gamma_5)] ,$$

which is compatible with the experimental results to within the accuracy of the measurements. Although the proportionality relation (24) seems to be verified, a problem arises for interpreting the absolute magnitude of the shifts. The observed difference

$$D(\Gamma_1) - D(\Gamma_5) = S(\Gamma_1) - S(\Gamma_5) \simeq 0.07 \text{ mm s}^{-1}$$

corresponds to a variation $\Delta E_c \simeq 100$ cm^{-1} of the kinetic energy of the emitting nucleus between the states $|\Gamma_1\rangle$ and $|\Gamma_5\rangle$. This value seems quite large at first, considering that the energy of the vibrational mode used in the calculation is only $\hbar\omega_e \simeq 70$ cm^{-1}, and that the vibronic states $|\Gamma_1\rangle$ and $|\Gamma_5\rangle$ differ by a fraction of $\hbar\omega_e$, because of the different one (or two) phonon function admixtures in the two levels. But in fact the link between the motion of the emitting nucleus ^{57}Fe and the vibronic properties of the Fe^{2+} Jahn-Teller system is not so straightforward. In the classical or molecular picture, the Jahn-Teller ion is located at the center of a tetrahedron of neighboring atoms (S^{2-}) and the normal vibrational modes concern the motion of the neighbors, not of the central ion. For the opposite view, the extended picture of the lattice phonon TA(L) corresponds to a motion of the Zn^{2+} sublattice and therefore of the substituted Mössbauer ion. Further theoretical investigations are necessary in order to more completely exploit the isomer shift measurements which give unique information on the motion of the Jahn-Teller ion itself in different vibronic levels.

VI. CONCLUSION

The whole interpretation of the Mössbauer emission spectra of the Fe^{2+} ions in the source ZnS: ^{57}Co below 5 K is based upon the assignment of the two quadrupole doublets, respectively, to the excited spin-orbit levels Γ_4 and Γ_5, both with populations out of the thermal equilibrium. While direct evidence concerning the assignment of the external quadrupole doublet to the Γ_4 level was provided by the relaxation study in the absorber experiments (see part I), no such direct evidence existed for assigning the internal doublet to the level Γ_5. This assignment could have been initially questioned as differences between the isomer shift values and between the quadrupole splitting values of the Γ_4 and Γ_5 contributions were not predicted by the vibronic model presented by Ham in Ref. 4. However we have shown that such differences are expected when the overall spin-orbit separation of the ^5E state of Fe^{2+} is not much smaller than the vibrational energy. The present vibronic calculation shows that a moderate Jahn-Teller coupling between the ^5E state of Fe^{2+} and the low-energy TA(L) phonon of the ZnS matrix can account for the very different quadrupole interactions which are observed in the Γ_4 and Γ_5 levels, while still remaining compatible with the previous optical data on the system ZnS:Fe^{2+}. So this calculation fully supports the assignment of the internal quadrupole doublet to the Γ_5 level. It should be noted in addition that no other plausible assignment of this doublet can be made to any other zero phonon vibronic level originating from the ^5E state.

As a general conclusion the present study (Parts I and II) has demonstrated the possibility of observing hyperfine structures coming from metastable electronic levels populated by the radioactive decay in Mössbauer emission spectroscopy.

The interest of such experiments was further enhanced by the existence of a dynamical Jahn-Teller coupling in the case of ZnS:Fe^{2+}. The observation of hyperfine structures in two metastable levels in this system enabled a separate evaluation of the Jahn-Teller effect and of the covalency effect within the ^5E multiplet of the Fe^{2+} ion to be made.

Some possible extensions of the present work in the field of the Jahn-Teller coupling can be suggested. It would be interesting first to carry out Mössbauer emission experiments on a CdTe: ^{57}Co source and to compare the results with the predictions resulting from Vallin's calculation in the system CdTe:Fe^{2+} (Ref. 5). A difficulty exists however due to the absence of data concerning the reference value $6|C_E|$ of the maximum quadrupole interaction of Fe^{2+} in this matrix where covalency effects are important.

The extension of the present study to the hexagonal phase of ZnS (wurtzite) would be interesting with regard to possible modifications in the Jahn-Teller coupling of Fe^{2+} compared to that in the cubic phase (blende).

In the system CaF_2:Fe^{2+} where a large quadrupole splitting $\Delta E_Q(\Gamma_4) = 3.74$ mm s^{-1} has already been observed from absorber measurements,[17] the dynamical Jahn-Teller perturbation is probably very small. Further experiments on a CaF_2: ^{57}Co Mössbauer source should enable the second $\Delta E_Q(\Gamma_5)$ quadrupole splitting to be measured, in order to verify that it does not differ much from $\Delta E_Q(\Gamma_4)$, in contrast to the case of the system ZnS:Fe^{2+}.

Finally it would be worthwhile developing the theoretical interpretation of the second-order Doppler shift data in such Jahn-Teller systems, as these measurements enable the kinetic energy of the Jahn-Teller atom to be compared in different vibronic levels.

---

[*] Institut de Physique, Université de Liège, Sart-Tilman, B-4000, Liège, Belgique.

[1] G. A. Slack, S. Roberts, and F. S. Ham, Phys. Rev. 155, 170 (1967).

[2] J. T. Vallin, G. A. Slack, and C. C. Bradley, Phys. Rev. B 2, 4406 (1970).

[3] F. S. Ham and G. A. Slack, Phys. Rev. B 4, 777 (1971).

[4] F. S. Ham, J. Phys. (Paris) Suppl. 35, C6-121 (1974).

[5] J. T. Vallin, Phys. Rev. B 2, 2390 (1970).

[6] A. Gérard, P. Imbert, H. Prange, F. Varret, and M. Wintenberger, J. Phys. Chem. Solids 32, 2091 (1971).

[7] C. Garcin, P. Imbert, and G. Jéhanno, Solid State Commun. 21, 545 (1977).

[8] G. A. Slack, S. Roberts, and J. T. Vallin, Phys. Rev. 187, 511 (1969).

[9] P. Imbert, C. Garcin, G. Jéhanno, and A. Gérard, in *Inter-*

national Conference on Mössbauer Spectroscopy, Bucharest, 1977, edited by D. Barb and D. Tarina (Central Institute of Physics, Bucharest, Romania, 1977), Vol. II, p. 123.

[10] G. F. Koster, J. O. Dimmock, R. G. Wheeler, and H. Statz, *Properties of the Thirty-Two Point Groups* (MIT Press, Cambridge, Mass., 1963).

[11] F. S. Ham, Phys. Rev. B 4, 3854 (1971).

[12] F. S. Ham, in *Electron Paramagnetic Resonance,* edited by S. Geschwind (Plenum, New York, 1971).

[13] A. L. Natadze and A. I. Ryskin, Solid State Commun. 24, 147 (1977); Phys. Status Solidi B 97, 175 (1980).

[14] G. A. Slack, F. S. Ham, and R. M. Chrenko, Phys. Rev. 152, 376 (1966).

[15] F. S. Ham, Phys. Rev. 166, 307 (1967).

[16] H. Frauenfelder, *The Mössbauer Effect* (Benjamin, New York, 1962), p. 63.

[17] J. R. Régnard and U. Dürr, J. Phys. (Paris) 40, 997 (1979).